Draft dated June 5, 2008

Circulation restricted to LIGO-I members

All-sky LIGO Search for Periodic Gravitational Waves in the Early S5 Data

Proposed journal: Physical Review Letters

B. Abbott,[16] R. Abbott,[16] R. Adhikari,[16] P. Ajith,[2] B. Allen,[2,54] G. Allen,[32] R. Amin,[20] S. B. Anderson,[16] W. G. Anderson,[54] M. A. Arain,[41] M. Araya,[16] H. Armandula,[16] P. Armor,[54] Y. Aso,[10] S. Aston,[40] P. Aufmuth,[15] C. Aulbert,[2] S. Babak,[1] S. Ballmer,[16] H. Bantilan,[8] B. C. Barish,[16] C. Barker,[18] D. Barker,[18] B. Barr,[42] P. Barriga,[53] M. A. Barton,[42] M. Bastarrika,[42] K. Bayer,[17] J. Betzwieser,[16] P. T. Beyersdorf,[28] I. A. Bilenko,[23] G. Billingsley,[16] R. Biswas,[54] E. Black,[16] K. Blackburn,[16] L. Blackburn,[17] D. Blair,[53] B. Bland,[18] T. P. Bodiya,[17] L. Bogue,[19] R. Bork,[16] V. Boschi,[16] S. Bose,[55] P. R. Brady,[54] V. B. Braginsky,[23] J. E. Brau,[47] M. Brinkmann,[2] A. Brooks,[16] D. A. Brown,[33] G. Brunet,[17] A. Bullington,[32] A. Buonanno,[43] O. Burmeister,[2] R. L. Byer,[32] L. Cadonati,[44] G. Cagnoli,[42] J. B. Camp,[24] J. Cannizzo,[24] K. Cannon,[16] J. Cao,[17] L. Cardenas,[16] S. Caride,[8] T. Casebolt,[32] G. Castaldi,[50] C. Cepeda,[16] E. Chalkley,[42] P. Charlton,[9] S. Chatterji,[16] S. Chelkowski,[40] Y. Chen,[6,1] N. Christensen,[8] D. Clark,[32] J. Clark,[42] T. Cokelaer,[7] R. Conte,[49] D. Cook,[18] T. Corbitt,[17] D. Coyne,[16] J. D. E. Creighton,[54] A. Cumming,[42] L. Cunningham,[42] R. M. Cutler,[40] J. Dalrymple,[33] K. Danzmann,[15,2] G. Davies,[7] D. DeBra,[32] J. Degallaix,[1] M. Degree,[32] V. Dergachev,[45] S. Desai,[34] R. DeSalvo,[16] S. Dhurandhar,[14] M. Díaz,[36] J. Dickson,[4] A. Dietz,[7] F. Donovan,[17] K. L. Dooley,[41] E. E. Doomes,[31] R. W. P. Drever,[5] I. Duke,[17] J.-C. Dumas,[53] R. J. Dupuis,[16] J. G. Dwyer,[10] C. Echols,[16] A. Effler,[18] P. Ehrens,[16] G. Ely,[8] E. Espinoza,[16] T. Etzel,[16] T. Evans,[19] S. Fairhurst,[7] Y. Fan,[53] D. Fazi,[16] H. Fehrmann,[2] M. M. Fejer,[32] L. S. Finn,[34] K. Flasch,[54] N. Fotopoulos,[54] A. Freise,[40] R. Frey,[47] T. Fricke,[16,48] P. Fritschel,[17] V. V. Frolov,[19] M. Fyffe,[19] J. Garofoli,[18] I. Gholami,[1] J. A. Giaime,[19,20] S. Giampanis,[48] K. D. Giardina,[19] K. Goda,[17] E. Goetz,[45] L. Goggin,[16] G. González,[20] S. Gossler,[2] R. Gouaty,[20] A. Grant,[42] S. Gras,[53] C. Gray,[18] M. Gray,[4] R. J. S. Greenhalgh,[27] A. M. Gretarsson,[11] F. Grimaldi,[17] R. Grosso,[36] H. Grote,[2] S. Grunewald,[1] M. Guenther,[18] E. K. Gustafson,[16] R. Gustafson,[45] B. Hage,[15] J. M. Hallam,[40] D. Hammer,[54] C. Hanna,[20] J. Hanson,[19] J. Harms,[2] G. Harry,[17] E. Harstad,[47] K. Hayama,[36] T. Hayler,[27] J. Heefner,[16] I. S. Heng,[42] M. Hennessy,[32] A. Heptonstall,[42] M. Hewitson,[2] S. Hild,[40] E. Hirose,[33] D. Hoak,[19] D. Hosken,[39] J. Hough,[42] S. H. Huttner,[42] D. Ingram,[18] M. Ito,[47] A. Ivanov,[16] B. Johnson,[18] W. W. Johnson,[20] D. I. Jones,[51] G. Jones,[7] R. Jones,[42] L. Ju,[53] P. Kalmus,[10] V. Kalogera,[26] S. Kamat,[10] J. Kanner,[43] D. Kasprzyk,[40] E. Katsavounidis,[17] K. Kawabe,[18] S. Kawamura,[25] F. Kawazoe,[25] W. Kells,[16] D. G. Keppel,[16] F. Ya. Khalili,[23] R. Khan,[10] E. Khazanov,[13] C. Kim,[26] P. King,[16] J. S. Kissel,[20] S. Klimenko,[41] K. Kokeyama,[25] V. Kondrashov,[16] R. K. Kopparapu,[34] D. Kozak,[16] I. Kozhevatov,[13] B. Krishnan,[1] P. Kwee,[15] P. K. Lam,[4] M. Landry,[18] M. M. Lang,[34] B. Lantz,[32] A. Lazzarini,[16] M. Lei,[16] N. Leindecker,[32] V. Leonhardt,[25] I. Leonor,[47] K. Libbrecht,[16] H. Lin,[41] P. Lindquist,[16] N. A. Lockerbie,[52] D. Lodhia,[40] M. Lormand,[19] P. Lu,[32] M. Lubinski,[18] A. Lucianetti,[41] H. Lück,[15,2] B. Machenschalk,[2] M. MacInnis,[17] M. Mageswaran,[16] K. Mailand,[16] V. Mandic,[46] S. Márka,[10] Z. Márka,[10] A. Markosyan,[32] J. Markowitz,[17] E. Maros,[16] I. Martin,[42] R. M. Martin,[41] J. N. Marx,[16] K. Mason,[17] F. Matichard,[20] L. Matone,[10] R. Matzner,[35] N. Mavalvala,[17] R. McCarthy,[18] D. E. McClelland,[4] S. C. McGuire,[31] M. McHugh,[22] G. McIntyre,[16] G. McIvor,[35] D. McKechan,[7] K. McKenzie,[4] T. Meier,[15] A. Melissinos,[48] G. Mendell,[18] R. A. Mercer,[41] S. Meshkov,[16] C. J. Messenger,[2] D. Meyers,[16] J. Miller,[42,16] J. Minelli,[34] S. Mitra,[14] V. P. Mitrofanov,[23] G. Mitselmakher,[41] R. Mittleman,[17] O. Miyakawa,[16] B. Moe,[54] S. Mohanty,[36] G. Moreno,[18] K. Mossavi,[2] C. MowLowry,[4] G. Mueller,[41] S. Mukherjee,[36] H. Mukhopadhyay,[14] H. Müller-Ebhardt,[2] J. Munch,[39] P. Murray,[42] E. Myers,[18] J. Myers,[18] T. Nash,[16] J. Nelson,[42] G. Newton,[42] A. Nishizawa,[25] K. Numata,[24] J. O'Dell,[27] G. Ogin,[16] B. O'Reilly,[19] R. O'Shaughnessy,[34] D. J. Ottaway,[17] R. S. Ottens,[41] H. Overmier,[19] B. J. Owen,[34] Y. Pan,[43] C. Pankow,[41] M. A. Papa,[1,54] V. Parameshwaraiah,[18] P. Patel,[16] M. Pedraza,[16] S. Penn,[12] A. Perreca,[40] T. Petrie,[34] I. M. Pinto,[50] M. Pitkin,[42] H. J. Pletsch,[2] M. V. Plissi,[42] F. Postiglione,[49] M. Principe,[50] R. Prix,[2] V. Quetschke,[41] F. Raab,[18] D. S. Rabeling,[4] H. Radkins,[18] N. Rainer,[2] M. Rakhmanov,[30] M. Ramsunder,[34] H. Rehbein,[2] S. Reid,[42] D. H. Reitze,[41] R. Riesen,[19] K. Riles,[45] B. Rivera,[18] N. A. Robertson,[16,42] C. Robinson,[7] E. L. Robinson,[40] S. Roddy,[19] A. Rodriguez,[20] A. M. Rogan,[55] J. Rollins,[10] J. D. Romano,[36] J. Romie,[19] R. Route,[32] S. Rowan,[42] A. Rüdiger,[2] L. Ruet,[17] P. Russell,[16] K. Ryan,[18] S. Sakata,[25] M. Samidi,[16] L. Sancho de la Jordana,[38] V. Sandberg,[18] V. Sannibale,[16] S. Saraf,[29] P. Sarin,[17] B. S. Sathyaprakash,[7] S. Sato,[25] P. R. Saulson,[33] R. Savage,[18] P. Savov,[6] S. W. Schediwy,[53] R. Schilling,[2] R. Schnabel,[2] R. Schofield,[47] B. F. Schutz,[1,7] P. Schwinberg,[18] S. M. Scott,[4] A. C. Searle,[4] B. Sears,[16] F. Seifert,[2] D. Sellers,[19] A. S. Sengupta,[16] P. Shawhan,[43] D. H. Shoemaker,[17] A. Sibley,[19] X. Siemens,[54]

D. Sigg,[18] S. Sinha,[32] A. M. Sintes,[38,1] B. J. J. Slagmolen,[4] J. Slutsky,[20] J. R. Smith,[33] M. R. Smith,[16] N. D. Smith,[17] K. Somiya,[2,1] B. Sorazu,[42] L. C. Stein,[17] A. Stochino,[16] R. Stone,[36] K. A. Strain,[42] D. M. Strom,[47] A. Stuver,[19] T. Z. Summerscales,[3] K.-X. Sun,[32] M. Sung,[20] P. J. Sutton,[7] H. Takahashi,[1] D. B. Tanner,[41] R. Taylor,[16] R. Taylor,[42] J. Thacker,[19] K. A. Thorne,[34] K. S. Thorne,[6] A. Thüring,[15] K. V. Tokmakov,[42] C. Torres,[19] C. Torrie,[42] G. Traylor,[19] M. Trias,[38] W. Tyler,[16] D. Ugolini,[37] J. Ulmen,[32] K. Urbanek,[32] H. Vahlbruch,[15] C. Van Den Broeck,[7] M. van der Sluys,[26] S. Vass,[16] R. Vaulin,[54] A. Vecchio,[40] J. Veitch,[40] P. Veitch,[39] A. Villar,[16] C. Vorvick,[18] S. P. Vyachanin,[23] S. J. Waldman,[16] L. Wallace,[16] H. Ward,[42] R. Ward,[16] M. Weinert,[2] A. Weinstein,[16] R. Weiss,[17] S. Wen,[20] K. Wette,[4] J. T. Whelan,[1] S. E. Whitcomb,[16] B. F. Whiting,[41] C. Wilkinson,[18] P. A. Willems,[16] H. R. Williams,[34] L. Williams,[41] B. Willke,[15,2] I. Wilmut,[27] W. Winkler,[2] C. C. Wipf,[17] A. G. Wiseman,[54] G. Woan,[42] R. Wooley,[19] J. Worden,[18] W. Wu,[41] I. Yakushin,[19] H. Yamamoto,[16] Z. Yan,[53] S. Yoshida,[30] M. Zanolin,[11] J. Zhang,[45] L. Zhang,[16] C. Zhao,[53] N. Zotov,[21] M. Zucker,[17] and J. Zweizig[16]

(The LIGO Scientific Collaboration, http://www.ligo.org)

[1] *Albert-Einstein-Institut, Max-Planck-Institut für Gravitationsphysik, D-14476 Golm, Germany*
[2] *Albert-Einstein-Institut, Max-Planck-Institut für Gravitationsphysik, D-30167 Hannover, Germany*
[3] *Andrews University, Berrien Springs, MI 49104 USA*
[4] *Australian National University, Canberra, 0200, Australia*
[5] *California Institute of Technology, Pasadena, CA 91125, USA*
[6] *Caltech-CaRT, Pasadena, CA 91125, USA*
[7] *Cardiff University, Cardiff, CF24 3AA, United Kingdom*
[8] *Carleton College, Northfield, MN 55057, USA*
[9] *Charles Sturt University, Wagga Wagga, NSW 2678, Australia*
[10] *Columbia University, New York, NY 10027, USA*
[11] *Embry-Riddle Aeronautical University, Prescott, AZ 86301 USA*
[12] *Hobart and William Smith Colleges, Geneva, NY 14456, USA*
[13] *Institute of Applied Physics, Nizhny Novgorod, 603950, Russia*
[14] *Inter-University Centre for Astronomy and Astrophysics, Pune - 411007, India*
[15] *Leibniz Universität Hannover, D-30167 Hannover, Germany*
[16] *LIGO - California Institute of Technology, Pasadena, CA 91125, USA*
[17] *LIGO - Massachusetts Institute of Technology, Cambridge, MA 02139, USA*
[18] *LIGO Hanford Observatory, Richland, WA 99352, USA*
[19] *LIGO Livingston Observatory, Livingston, LA 70754, USA*
[20] *Louisiana State University, Baton Rouge, LA 70803, USA*
[21] *Louisiana Tech University, Ruston, LA 71272, USA*
[22] *Loyola University, New Orleans, LA 70118, USA*
[23] *Moscow State University, Moscow, 119992, Russia*
[24] *NASA/Goddard Space Flight Center, Greenbelt, MD 20771, USA*
[25] *National Astronomical Observatory of Japan, Tokyo 181-8588, Japan*
[26] *Northwestern University, Evanston, IL 60208, USA*
[27] *Rutherford Appleton Laboratory, Chilton, Didcot, Oxon OX11 0QX United Kingdom*
[28] *San Jose State University, San Jose, CA 95192, USA*
[29] *Sonoma State University, Rohnert Park, CA 94928, USA*
[30] *Southeastern Louisiana University, Hammond, LA 70402, USA*
[31] *Southern University and A&M College, Baton Rouge, LA 70813, USA*
[32] *Stanford University, Stanford, CA 94305, USA*
[33] *Syracuse University, Syracuse, NY 13244, USA*
[34] *The Pennsylvania State University, University Park, PA 16802, USA*
[35] *The University of Texas at Austin, Austin, TX 78712, USA*
[36] *The University of Texas at Brownsville and Texas Southmost College, Brownsville, TX 78520, USA*
[37] *Trinity University, San Antonio, TX 78212, USA*
[38] *Universitat de les Illes Balears, E-07122 Palma de Mallorca, Spain*
[39] *University of Adelaide, Adelaide, SA 5005, Australia*
[40] *University of Birmingham, Birmingham, B15 2TT, United Kingdom*
[41] *University of Florida, Gainesville, FL 32611, USA*
[42] *University of Glasgow, Glasgow, G12 8QQ, United Kingdom*
[43] *University of Maryland, College Park, MD 20742 USA*
[44] *University of Massachusetts, Amherst, MA 01003 USA*
[45] *University of Michigan, Ann Arbor, MI 48109, USA*
[46] *University of Minnesota, Minneapolis, MN 55455, USA*
[47] *University of Oregon, Eugene, OR 97403, USA*
[48] *University of Rochester, Rochester, NY 14627, USA*
[49] *University of Salerno, 84084 Fisciano (Salerno), Italy*

[50] University of Sannio at Benevento, I-82100 Benevento, Italy
[51] University of Southampton, Southampton, SO17 1BJ, United Kingdom
[52] University of Strathclyde, Glasgow, G1 1XQ, United Kingdom
[53] University of Western Australia, Crawley, WA 6009, Australia
[54] University of Wisconsin-Milwaukee, Milwaukee, WI 53201, USA
[55] Washington State University, Pullman, WA 99164, USA
(Dated: June 5, 2008)

We report on an all-sky search with the LIGO detectors for periodic gravitational waves in the frequency range 50 – 1100 Hz and with the frequency's time derivative in the range -5×10^{-9} – 0 Hz s^{-1}. Data from the first eight months of the fifth LIGO science run (S5) have been used in this search, which is based on a semi-coherent method (PowerFlux) of summing strain power. Observing no evidence of periodic gravitational radiation, we report 95% confidence-level upper limits on radiation emitted by isolated rotating neutron stars within the search range. Strain limits below 10^{-24} are obtained near 100 Hz, and the improvement over previous searches increases the spatial volume sampled by approximately 100 over the search band. The best range obtained is at the highest frequency, 1100Hz, *i.e.*, about 500pc for a neutron star with equatorial ellipticity 10^{-6}.

PACS numbers: 04.80.Nn, 95.55.Ym, 97.60.Gb, 07.05.Kf

I. INTRODUCTION

We have carried out an all-sky search with the LIGO (Laser Interferometer Gravitational-wave Observatory) detectors [1, 2] for periodic gravitational waves, using data from the first eight months of LIGO's fifth science run (S5). We have searched over the frequency range 50 – 1100 Hz, allowing for a frequency time derivative in the range -5×10^{-9} – 0 Hz s^{-1}. Rotating neutron stars in our galaxy are the prime target. At signal frequencies near 100 Hz we obtain strain sensitivities below 10^{-24}, a strain at which one might optimistically expect to see the strongest signal from a previously unknown neutron star according to a generic argument originally made by Blandford (unpublished), extended in our previous search for such objects in S2 data [3], but recently refined to give less optimistic estimates [4].

Using data from earlier science runs, the LIGO Scientific Collaboration (LSC) has previously reported on targeted searches for periodic gravitational radiation from known pulsars [5, 6, 7, 8] and from the low-mass X-ray binary system Scorpius X-1 [3, 9]; and on all-sky searches for unknown rotating neutron stars (henceforth designated as "pulsars" here). The all-sky searches have been performed using a short-period coherent search in the 160.0 – 728.8 Hz frequency range [3], and using a long-period semi-coherent search in the 200 – 400 Hz frequency range [10] in the S2 data and the 50 – 1000 Hz range in the S4 data [11]. Einstein@Home, a distributed home computing effort [12], has also been running searches using a coherent first stage, followed by a simple coincidence stage [13], for which S3 and S4 results have been posted [13, 14].

The data collected in the S5 data run were more sensitive than in previous data runs, and the amount of data reported here is an increase by a factor of eight over that reported from the S4 data run [11], resulting in upper limits on periodic gravitational waves about a factor of 3-6 lower than those from the S4 data, depending on source frequency. This improvement gives an increase in sampled galactic volume by about a factor of 100, depending on the assumed source frequency and spin-down. At a signal frequency of 1100 Hz we achieve sensitivity to neutron stars of equatorial ellipticity $\epsilon \sim 10^{-6}$ at distances up to 500 pc [11]. For reference, there are about 25 known pulsars within 500 pc, half of which have rotation frequencies compatible with the LIGO band (although none has a frequency derivative large enough to suggest detectability via gravitational waves[15]).

II. THE LIGO DETECTORS AND THE S5 SCIENCE RUN

The LIGO detector network consists of a 4-km interferometer in Livingston Louisiana, (L1), and two interferometers in Hanford Washington, one 4-km and another 2-km (H1 and H2).

The data analyzed in this paper were produced in the first eight months of LIGO's fifth science run (S5). This run started at 16:00 UTC on November 4, 2005 at the LIGO Hanford Observatory and at 16:00 UTC on November 14, 2005 at the LIGO Livingston Observatory; the run ended at 00:00 UTC on October 1, 2007. During this run, all three LIGO detectors had displacement spectral amplitudes very near their design goals of $1.1 \times 10^{-19}\,\mathrm{m\,Hz^{-1/2}}$ [16] in their most sensitive frequency band near 150 Hz (the H2 strain sensitivity was roughly a factor of two worse than that of the other interferometers; its data were not used in this search).

The data were acquired and digitized at a rate of 16384 Hz. Data acquisition was periodically interrupted by disturbances such as seismic transients (natural or anthropogenic), reducing the net running time of the interferometers. In addition, there were 1–2 week commissioning breaks to repair equipment and address newly identified noise sources. The resulting duty factors for the interferometers were approximately 69% for H1, 77%

for H2, and 57% for L1 during the first eight months. A nearby construction project degraded the L1 duty factor significantly during this early period of the S5 run. By the end of the S5 run, the cumulative duty factors had improved to 78% for H1, 79% for H2, and 66% for L1.

III. SIGNAL WAVEFORMS

The general form of a gravitational-wave signal is described in terms of two orthogonal transverse polarizations defined to be "+" with waveform $h_+(t)$ and "×" with waveform $h_\times(t)$, for which separate and time-dependent antenna pattern factors F_+ and $F_\times$ apply, which depend on a polarization angle ψ [17]. For periodic gravitational waves, which in general are elliptically polarized, the individual components $h_{+,\times}$ have the form $h_+(t) = A_+ \cos\Phi(t)$ and $h_\times(t) = A_\times \sin\Phi(t)$, where A_+ and $A_\times$ are the amplitudes of the two polarizations, and $\Phi(t)$ is the phase of the signal at the detector. For the semi-coherent method used in this search, only the instantaneous signal frequency in the detector reference frame, $2\pi f(t) = d\Phi(t)/dt$, needs to be calculated. For an isolated, precession-free, rigidly rotating neutron star the quadrupolar amplitudes A_+ and $A_\times$ are related to wave amplitude, h_0, by $A_+ = h_0\frac{1+\cos^2\iota}{2}$ and $A_\times = h_0\cos\iota$, where ι describes the inclination angle of the star's spin axis with respect to the line of sight. For such a star, the signal wave frequency, f, is twice the rotation frequency, f_r.

The detector reference frame frequency $f(t)$ can, to a very good approximation, be related to the frequency $\hat{f}(t)$ in the Solar System Barycenter (SSB) frame by [10] $f(t) - \hat{f}(t) \simeq \hat{f}(t)\frac{\mathbf{v}(t)\cdot\mathbf{n}}{c}$, where $\mathbf{v}(t)$ is the detector's velocity with respect to the SSB frame, and $\mathbf{n}$ is the unit-vector pointing from the detector toward the sky-location of the source [10].

IV. ANALYSIS METHOD

The PowerFlux method used in this analysis is described in detail elsewhere [11] and is a variation upon the StackSlide method [18]. Here we summarize briefly its main features.

A strain power estimator is derived from summing measures of strain power from many short, 50%-overlap, Hann-windowed Fourier transforms (SFTs) that have been created from 30-minute intervals of calibrated strain data. In searching a narrow frequency range (0.5 mHz spacing) for an assumed source sky location, explicit corrections are made for Doppler modulations of the apparent source frequency. These modulations are due to the Earth's rotation and its orbital motion around the SSB, and the frequency's time derivative, $\dot{f}$, intrinsic to the source. Corrections are also applied for antenna pattern modulation, assuming five different polarizations: four linear polarizations separated by $\pi/8$ in polarization angle, and circular polarization. When summing, the variability of the noise is taken into account with an SFT-dependent weight proportional to the expected inverse variance of the background noise power (see [11] for detailed formulae). Initial data conditioning includes a noise decomposition algorithm described previously [11, 19] in which the noise variations within each 0.25-Hz band are fitted to a factorization of time-dependent and frequency-dependent coefficients with approximately Gaussian residuals.

The search range for initial frequency $\hat{f}_0$ values is 50 – 1100 Hz with a uniform grid spacing equal to the size of an SFT frequency bin [1/(30 min)]. The range of $\dot{f}$ values searched is -5×10^{-9}–0 Hz s^{-1} with a spacing of 5×10^{-10} Hz s^{-1}, since isolated rotating neutron stars are expected on average to spin down with time. As discussed in our previous reports [3, 10, 11], the number of sky points that must be searched grows quadratically with the frequency $\hat{f}_0$, ranging here from about five thousand at 50 Hz to about 2.4 million at 1100 Hz. The sky grid used here is isotropic and covers the entire sky.

Upper limits calculated in this method are strict frequentist limits on linear and circular polarization in small patches on the sky, with the limits quoted here being the highest limits in each 0.25-Hz band over broad regions of the sky. These are interpreted as limits on worst-case (linear polarization) and best-case (circular polarization) orientations of rotating neutron stars. It proved useful in the 1-month S4 data analysis to divide the sky into annular regions ("sky bands") centered upon the Sun's average direction during the S4 run, since directions orthogonal to this axis would have little Doppler modulation and hence be contaminated by stationary instrumental line artifacts [11, 19]. Since the eight months of data analyzed here cover a larger span of the Earth's orbit, such contamination affects only much smaller patches at the ecliptic poles (with small offsets depending on the presumed spin-down). A total of 0.6% of the search volume in sky location and spindown was excluded from the upper-limit analysis due to this effect.

The primary changes in the PowerFlux algorithm used in this search concern followup of outlier candidates. (The general method for setting upper limits is identical to that used in the S4 search [11].) Here we summarize the followup method used. Single-interferometer searches are carried out separately for the H1 and L1 interferometers, leading to the upper limits on strain shown in Figure 1 and discussed below. During the processing leading to the single-IFO limits, the sky is divided into ten arbitrary equal-area bands of right ascension (to reduce computer memory requirements) and into five bands of declination δ (equatorial, mid-north, polar-north, mid-south, and polar-south with boundaries at $\delta = \pm40.5°, \pm17.5°$) because of declination-dependence of run-averaged antenna pattern sensitivity. During determination of the maximum upper limit per sky region, per frequency band and per spin-down step, a "domain map" is constructed of local signal-to-noise ratio (SNR) maxima. First, the

SNR values obtained from all searched grid points are sorted. The grid points close (in right ascension, declination, and frequency) to the highest-SNR point are added to that point's domain and marked. The same procedure is then followed for the next highest-SNR grid point, creating a second domain, unless the point was already marked, in which case the older domain is enlarged. This procedure is followed until all grid points in the sky region have been assigned to domains. In this context, "close" is defined by the requirements that the angle between two template source directions is less than 3.1 times the characteristic angular resolution ($\simeq$8.3 mrad $\times$ 300 Hz / frequency) for that frequency band [11] and the frequencies of the two templates agree to within 3 SFT bins ($\simeq$1.7 mHz).

The 1000 domains with the highest maximum SNR are then re-analyzed to obtain improved estimates of the associated candidate parameters, using a modified gradient search with a matched filter to maximize SNR with respect to source frequency, spin-down, sky location, polarization angle ψ, and inclination angle ι [19]. This maximization step samples frequency and spin-down much more finely than in the initial search.

Often different candidates converge to similar parameters sets, especially when a strong disturbance is present. To expedite optimization we use a cache of existing computed candidates which is examined at each stage. If a higher-SNR candidate close in frequency, spin-down and sky location (but not orientation, which is usually poorly reconstructed) has been found already, the optimization process stops. The results (optimized parameters) of this maximization are then written to a log file for later post-processing.

When all sky regions and all spin-downs have been searched for a given 0.25 Hz band for both H1 and L1, the log files are compared in order to find coincidence between the two interferometers, where the following criteria are used to define candidates for followup analysis. The H1 and L1 candidates must each have an SNR value greater than 6.25, and they must agree in frequency to within 1/180 Hz = 5.56 mHz, in spin-down to within 4×10^{-10} Hz s^{-1}, and in sky location to within 0.14 radians. These conservative choices have been guided by simulated single-interferometer pulsar injections. Coincidence candidates within 0.1 Hz of one another are grouped together, since most candidates arise from detector spectral artifacts that become apparent upon manual investigation.

Candidates passing these criteria are subjected to a computationally intensive followup analysis that reproduces the all-sky PowerFlux search in a 0.25Hz band around each candidate, this time using the (incoherently) combined strain powers from both interferometers. Sky maps of strain and SNR are created and examined manually for each individual interferometer and for the combined interferometers. Spectral estimates from noise decomposition are also examined to identify possible artifacts leading to the coincident outliers.

In most cases strong but different spectral artifacts in the H1 and L1 detectors are found to account for the coincident candidates, where typically a wandering spectral line with a non-astrophysical modulation pattern but significantly higher power deposits enough strain energy in a template to exceed coincidence threshold. Often the combined H1-L1 SNR (for the same source template) is only slightly higher than or is even less than exceed othe higher of the two individual SNR's in the vicinity of the candidate or the combined SNR is only slightly improved, inconsistent with the astrophysical signal being sought.

V. RESULTS

The PowerFlux algorithm was applied to the first eight months of the S5 data from the H1 and L1 interferometers. Figure 1 shows the minima of the H1 and L1 95% confidence-level upper limits on pulsar gravitational wave amplitude h_0 for worst-case and best-case pulsar orientations for different declination bands (each with different run-averaged antenna pattern sensitivity). As in the S4 analysis, narrow bands around 60-Hz power mains harmonics, along with bands characterized by non-Gaussian noise, have been excluded from the displayed limits. Numerical values for frequencies and limits displayed in these figures can be obtained separately [20]. Systematic uncertainties on these values are dominated by calibration uncertainty at the $\sim$10% level.

All outliers were checked for coincidence between H1 and L1, as described above. In most cases single-interferometer spectral artifacts were readily found upon initial inspection, most of which had known instrumental or environmental sources, such as mechanical resonances ("violin modes") of the wires supporting interferometer mirrors, and power mains harmonics of 60 Hz. Other outliers were tracked down to previously unknown electromagnetic disturbances. For six coincidence candidates, no instrumental spectral artifacts were apparent. Their 0.1-Hz bands and favored spin-down values are listed in Table I, along with the maximum SNR's observed in H1 and L1 data.

None of these six candidates was confirmed, however, as a detection of a constant-amplitude, constant-spin-down periodic source of gravitational radiation. In each case, the combined H1-L1 SNR did not increase by more than 0.6 (0.4) units over the minimum (maximum) of the single-interferometer SNR's, with four candidates showing a *decrease* for combined SNR. Software simulations indicate that combined SNR should typically show an increase over minimum SNR by more than 2.0 units for a single-interferometer SNR threshold of 6.25. Hence we conservatively veto any candidate with an SNR increase less than 1 unit. In addition, manual exploration of these candidates was carried out, using larger portions of the S5 run's data, to determine whether SNR increased with increased data, and with subsets of the the original 8-month data, to determine whether a transient astrophys-

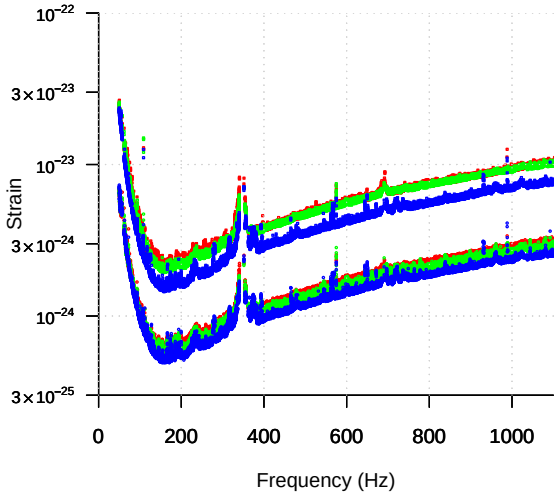

FIG. 1: Minimum (H1 or L1) upper limits on pulsar gravitational wave amplitude h_0 for the equatorial (red), intermediate (green), and polar (blue) declination bands for best-case (lower curves) and worst-case (upper curves) pulsar orientations. Shown are all the minimum limits for each of the 11 spin-down values from $-5 \times 10^{-9}\mathrm{Hzs}^{-1}$ to zero in steps of $5 \times 10^{-10}\mathrm{Hz\,s}^{-1}$.

ical source could explain the candidate. None of these explorations proved fruitful.

We also note that multi-interferometer injections indicate that for signal frequencies above 850 Hz, the coincidence requirements in frequency and sky location could be tightened by a factor of five to 1 mHz and by a factor of seven to 0.02 radians, respectively, with only a slight reduction in efficiency. None of the candidates in Table I satisfies these tighter criteria.

In summary, we have set upper limits on the strength of continuous-wave gravitational radiation using a semi-coherent method for summing of strain power from the LIGO interferometers. Strict frequentist upper limits have been derived over nearly the entire sky on linear and circular polarization amplitudes, corresponding to least favorable and most favorable pulsar orientations, respectively. Follow-up analysis of coincidence candidates with SNR > 6.25 did not yield a detection.

VI. ACKNOWLEDGMENTS

The authors gratefully acknowledge the support of the United States National Science Foundation for the construction and operation of the LIGO Laboratory and the Science and Technology Facilities Council of the United Kingdom, the Max-Planck-Society, and the State of Niedersachsen/Germany for support of the construction and operation of the GEO600 detector. The authors also gratefully acknowledge the support of the research by these agencies and by the Australian Research Council, the Council of Scientific and Industrial Research of India, the Istituto Nazionale di Fisica Nucleare of Italy, the Spanish Ministerio de Educacion y Ciencia, the Conselleria d'Economia Hisenda i Innovacio of the Govern de les Illes Balears, the Scottish Funding Council, the Scottish Universities Physics Alliance, The National Aeronautics and Space Administration, the Carnegie Trust, the Leverhulme Trust, the David and Lucile Packard Foundation, the Research Corporation, and the Alfred P. Sloan Foundation. This document has been assigned LIGO Laboratory document number LIGO-P080024-01-Z.

[1] A. Abramovici *et al.*, Science **256**, 325 (1992).
[2] B. Barish and R. Weiss, Phys. Today **52**, 44 (1999).
[3] B. Abbott *et al.* (The LIGO Scientific Collaboration), Phys. Rev. D **76**, 082001 (2007).
[4] B. Knispel and B. Allen, preprint arXiv:0804.3075 [gr-qc].
[5] B. Abbott *et al.* (The LIGO Scientific Collaboration), Phys. Rev. D **69**, 082004 (2004).
[6] B. Abbott *et al.* (The LIGO Scientific Collaboration), Phys. Rev. Lett. **94**, 181103 (2005).
[7] B. Abbott *et al.* (The LIGO Scientific Collaboration), M. Kramer, and A. G. Lyne, Phys. Rev. D **76**, 042001 (2007).
[8] B. Abbott *et al.* (The LIGO Scientific Collaboration), preprint arXiv:0805.4758 [gr-qc].
[9] B. Abbott *et al.* (The LIGO Scientific Collaboration), Phys. Rev. D **76**, 082003 (2007).
[10] B. Abbott *et al.* (The LIGO Scientific Collaboration), Phys. Rev. D **72**, 102004 (2005).
[11] B. Abbott *et al.* (The LIGO Scientific Collaboration), Phys. Rev. D **77**, 022001 (2008).
[12] The Einstein@Home project is built upon the BOINC (Berkeley Open Infrastructure for Network Computing) architecture described at `http://boinc.berkeley.edu/`.
[13] S3 results from the distributed computing project Einstein@Home can be found at `http://einstein.phys.uwm.edu/`.
[14] B. Abbott *et al.* (The LIGO Scientific Collaboration), preprint arXiv:0804.1747 [gr-qc].
[15] R. N. Manchester, G. B. Hobbs, A. Teoh and M. Hobbs, Astron. J. **129**, 1993 (2005). See also `http://www.atnf.csiro.au/research/pulsar/psrcat/`.
[16] B. Abbott *et al.* (The LIGO Scientific Collaboration), in preparation, preprint arXiv:0711.3041 [gr-qc].
[17] P. Jaranowski, A. Królak, and B.F. Schutz, Phys. Rev. D **58**, 063001 (1998).
[18] P. Brady, T. Creighton, Phys. Rev. D **61**, 082001 (2000)
[19] V. Dergachev, "Description of PowerFlux Algorithms

Frequency band (Hz)	Spin-down (Hz s^{-1})	H1 SNR	L1 SNR
867.2	-4.3×10^{-9}	6.27	6.30
941.0	-2.0×10^{-9}	6.50	6.67
967.8	-1.5×10^{-9}	6.26	6.33
979.5	-5.0×10^{-9}	6.40	6.29
1058.6	-5.0×10^{-10}	6.83	6.38
1070.2	-3.0×10^{-10}	6.72	6.99

TABLE I: List of coincidence candidates for which no instrumental spectral artifacts were observed.

and Implementation", LIGO technical document LIGO-T050186 (2005), available in
`http://admdbsrv.ligo.caltech.edu/dcc/`

[20] See EPAPS Document No. [number will be inserted by publisher] for numerical values of upper limits derived for the H1 and L1 interferometers in 0.25-Hz bands in the range 50-1000 Hz.